
Advanced Composite Materials
Publication details, including instructions for authors and subscription information:
http://www.tandfonline.com/loi/tacm20

# Cost-effective bridge girder strengthening using vacuum-assisted resin transfer molding (VARTM)

Nasim Uddin , Uday Vaidya , Muhammad Shohel & J.C. Serrano-Perez

Version of record first published: 02 Apr 2012.

To cite this article: Nasim Uddin , Uday Vaidya , Muhammad Shohel & J.C. Serrano-Perez (2004): Cost-effective bridge girder strengthening using vacuum-assisted resin transfer molding (VARTM), Advanced Composite Materials, 13:3-4, 255-281

To link to this article: http://dx.doi.org/10.1163/1568551042580163

*Adv. Composite Mater.*, Vol. 13, No. 3-4, pp. 255–281 (2004)

Also available online - www.vsppub.com



# Cost-effective bridge girder strengthening using vacuum-assisted resin transfer molding (VARTM)

NASIM UDDIN [1,*], UDAY VAIDYA [2], MUHAMMAD SHOHEL [3] and J. C. SERRANO-PEREZ [4]

[1] *Department of Civil Engineering and Mechanics, University of Wiscousin — Milwaukee, 3200N Cramer Street, Milwaukee, WI 53211, USA*
[2] *BEC 358F, Department of Materials Science and Engineering, UAB School of Engineering, The University of Alabama at Birmingham, Birmingham, AL 35216, USA*
[3] *Department of Civil and Environmental Engineering, The University of Alabama at Birmingham, Birmingham, AL 35294-4440, USA*
[4] *Composite Materials Research Laboratory, Department of Materials Science and Engineering, The University of Alabama at Birmingham, Birmingham, AL 35216, USA*

Received 19 February 2004; accepted 23 July 2004

**Abstract**—The objective of this paper is to present the results of a demonstration project to apply externally bonded CFRP fabrics to retrofit a simple span prestressed concrete girder with improved repair and hardening techniques. The technique, Vacuum Assisted Resin Transfer Molding (VARTM), newly introduced to civil infrastructure was implemented in the field within two days without any traffic interruption. As an alternative to traditional hand lay up, VARTM has several processing advantages, like saving the processing time, uniform resin application, intimate contact between each layer of CFRP and concrete substrate ensuring good consolidation to remove void or dry spot, higher fiber volume fraction (about 70%) and greater wettability of the fiber, etc. The performance of the strengthened structures depends on the above potential factors to obtain high structural performance. VARTM uses single-sided molding technology to infuse resin over fabrics wrapping large structures such as bridge girders and saving tooling and processing time. Recently, the VARTM technique has been implemented in strengthening of an I-565 highway bridge girder in Huntsville, Alabama. Laboratory investigation included the construction of small concrete prisms to study the bonding behavior of Carbon Fiber Reinforced Polymer (CFRP) and strengthened concrete beams using VARTM to simulate the performance with and without strengthening. To the end, the process of field demonstration of this newly introduced technique to civil infrastructure has been presented.

*Keywords*: VARTM; bridge strengthening; CFRP; girder.

*To whom correspondence should be addressed. E-mail: nuddin@uwm.edu

## 1. INTRODUCTION

The Federal Highway Administration (FHWA) estimates that a significant proportion of bridges in USA, including Alabama, are structurally deficient or functionally obsolete. High-quality and expedient repair methods are necessary to enhance the service life of bridge structures, and simultaneously make them less vulnerable to vandalism and fire. Reinforced concrete bridge girders are the superstructure elements between the abutments and these can suffer from surface deterioration problems. Deterioration of concrete can occur as a result of structural cracks, corrosion of reinforcement, and freeze-thaw degradation. Cost-effective methods with potential for field implementation are required to address the issue of repair and strengthening of bridge structures. Numerous researchers have studied the behavior of FRP strengthened concrete beam and the Departments of Transportation (DOTs) across the USA have implemented the FRP strengthening techniques by hand lay-up process. Mayo *et al*. [1] applied bonded FRP-laminates to strengthen and lift load restriction from a simple span, reinforced concrete slab bridge, bridge G270, in Missouri for Missouri DOT. Kachlekev and Laylor [2] upgraded the capacity of the historic Horsetail Falls Bridge for Oregon DOT. Shahrooz *et al*. [3] examined four 76-year old T-reinforced beams and retrofitted a 45-year old, three-span reinforced concrete slab bridge for Ohio DOT. Besides these, there have been seismic upgradings of bridge columns for I-57 in Illinois, I-580 in Reno, Nevada and I-80 in Salt Lake City, Utah.

This paper presents a bridge strengthening case that was completed recently for an I-565 highway bridge girder that produced integrated structures such as concrete-FRP, with a cost-effective method. VARTM is an emerging manufacturing technique that holds promise as an affordable alternative to traditional autoclave molding and automated fiber placement for producing large-scale structural parts. It is a process currently widely used in automotive, boat industry and aerospace applications. It is ideal for large structures and suitable for field implementation. The use of a vacuum makes the resin application more uniform than with traditional hand lay-up, and has also proven to be environmentally friendly. This newly processing technique for bridge strengthening uses single-sided tooling, which results in significant savings in tooling costs, and vacuum-bag technology. This process has very attractive cost-advantages in comparison to hand lay-up impregnation methods. Other advantages of VARTM are low process volatile emission (and therefore environmentally safer), high fiber-to-resin ratio, good quality and process repeatability. As a result, savings in time, material and labor, and significant cost reduction are achieved in this case as compared to the traditional hand lay-up process. The next section gives details of the procedure of VARTM in concrete.

## 2. VARTM IN CONCRETE SPECIMENS

As an alternative to the labor intensive hand lay-up process, VARTM is an attractive process since it can save processing time (specially when many FRP layers are being

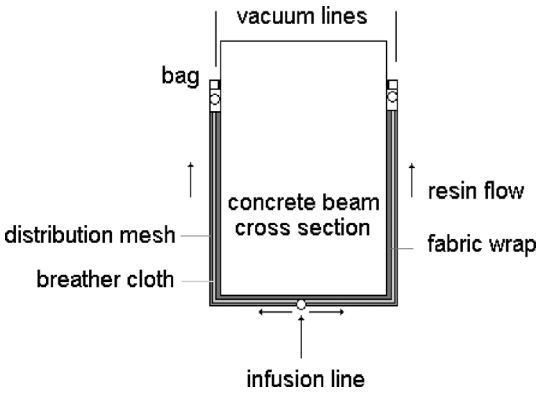


**Figure 1.** VARTM in rectangular concrete beam.



applied), makes the resin application more uniform than with traditional hand lay-up, and has also proven to be environmentally friendly since it produces no volatile organic compound (VOC) emissions. It is a process widely used in automotive and aerospace applications. The shortcomings of traditional lay-up techniques are: (i) the need for skilled workers to handle the fabric; (ii) improper wetting; (iii) difficulty in controlling long bridge girders and columns. On the other hand, VARTM is believed to form a strong uniform interface, free of resin-rich areas, without compromising the integrity of the fabric.

For this particular application, the surface of the concrete acts as the tool for the infusion process. After the surface of the concrete is prepared, a layer of primer is applied in the area to be infused. A vacuum seal is formed around the beam or column, using vacuum bag sealant tape to ensure an airtight seal. The dry fabric, initially cut to shape, is then placed on the concrete surface and held in place using adhesive tape on the edges. Then, the stretched fabric is covered using a porous medium, and a distribution mesh, to allow resin flow through the fabric. The infusion and vacuum lines are then placed, and finally covered by a bagging film. The lay-up is debulked and the resin/hardener mixture is infused with the aid of a vacuum. The feasibility of using VARTM was demonstrated on an 1828.8 mm (6 ft) RC beam, as illustrated in Figs 1 and 2. The resin flows across the fabric, and fills any surface flaw by the aid of the hydrostatic pressure that is applied by the atmosphere on the bag. The infusion parameters were optimized so that the infusion was symmetrical and even (Fig. 2), and resin rich areas were avoided. Curing took place under vacuum.

The main issues in the VARTM process are resin flow and maintaining the vacuum until the resin gets cured. Flow of resin is mainly affected by the permeability of the porous media, number of fiber layers and orientation of the fiber, resin viscosity and surface roughness of concrete. The resin flows across the fabric and follows Darcy's law given in equation (1):

$$J = -\frac{k}{\eta}\Delta P, \tag{1}$$

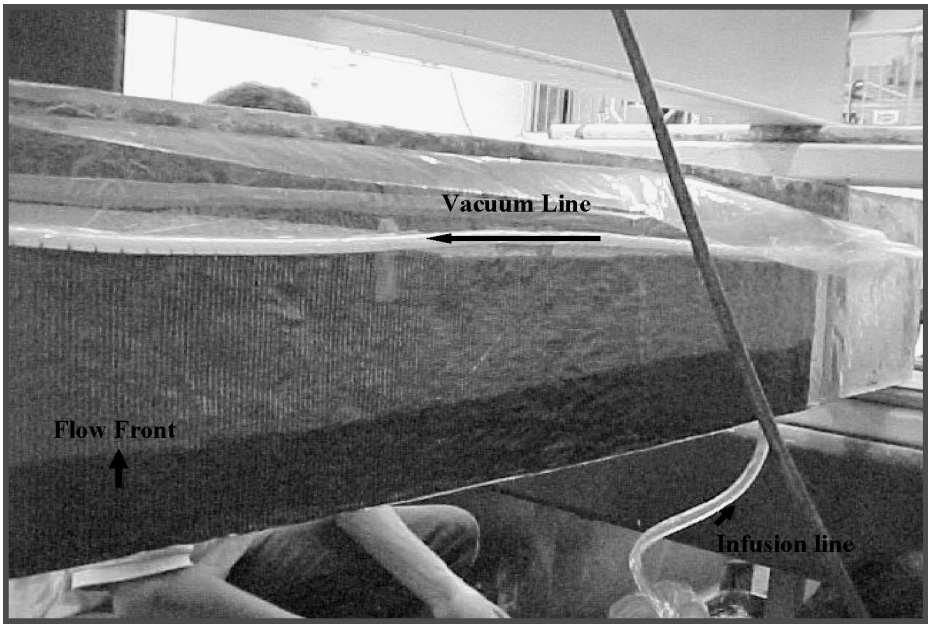


**Figure 2.** VARTM processing on 1828.8 mm (6 ft) RC beam.

where $J$ is the volume current density, $k$ is the permeability of the porous media, $\eta$ is the viscosity of the resin and $\Delta P$ is the applied pressure difference that drives the resin flow. When a homogenous material is injected with a resin, the filling time of the injection of a rectangular strip can be calculated using the same modified Darcy's law given in equation (2) [4]:

$$\textit{fill-time} = \frac{\phi \eta l^2}{2k\Delta P}, \tag{2}$$

where $l$ is flow distance (length of the strip). It is obvious from equation 2 that low viscosity resin is desired for a low injection time. The viscosity of the Sikadur 300 is 300 mPa.s and it was used for this purpose. The porosity of most reinforcements used is between 0.5 and 0.85 and the permeability could vary greatly. To obtain an approximation of the permeability of the reinforcement, the Carman-Kozney relation given in equation (3) [5] was used

$$k = \frac{d_f^2(1 - v_f)^3}{16K v_f^2}, \tag{3}$$

where $d_f$ is fiber diameter, $v_f$ is volume fraction, and $K$ is the Kozney constant. The Kozney constant for T-300 carbon is $K = 6.9$ [5], and T-300 fiber diameter $d_f = 7\ \mu$m. Solving for the experimentally obtained volume fraction, $k$ in the reinforcement is $2.21 \times 10^{-13}$ m$^2$. This value is very small and would require very long infusion time. So this factor was optimized by using a distribution mesh. A maximum pressure difference of 1 bar was used.

There were four steps involved in the VARTM process to achieve good strengthening: wetting/impregnation, lay-up, consolidation, and solidification. The desired area of the fiber can be wetted allowing minimum fill time given in equation (2) and making sure that the resin flows entirely all around the fiber. To ensure this, the location of the inlet/infusion lines and the number and location of vacuum lines in a designated area were designed.

## 3. CASE STUDY

### *3.1. I-565 highway bridge girder*

The bridge selected for demonstration of the VARTM strengthening technology is bridge I-565 highway located on Route/Bin 52 in Madison County. It is a 27.13 m (89 ft) long solid pre-stressed concrete girder, cast *in situ* slab bridge built in 1991. The bridge has a load restriction of 71.2 kN (16 kips) for HS20 trucks. After visiting the site of some cracked and deteriorated girders the authors and the Alabama Department of Transportation (ALDOT) selected this bridge girder for evaluation.

Figure 3 is the I-565 highway bridge in Huntsville. At the present condition it was seen that the open spaces in between some girders were sealed. As a result, cracks developed very close to the support due to bending caused by the temperature variation shown in Fig. 4 [6].

Table 1 shows the average seasonal temperatures variation in major cities in Alabama. The mean annual temperature could vary by 26/27°F (14/15°C).

**Figure 3.** I-565 highway bridge in Huntsville.

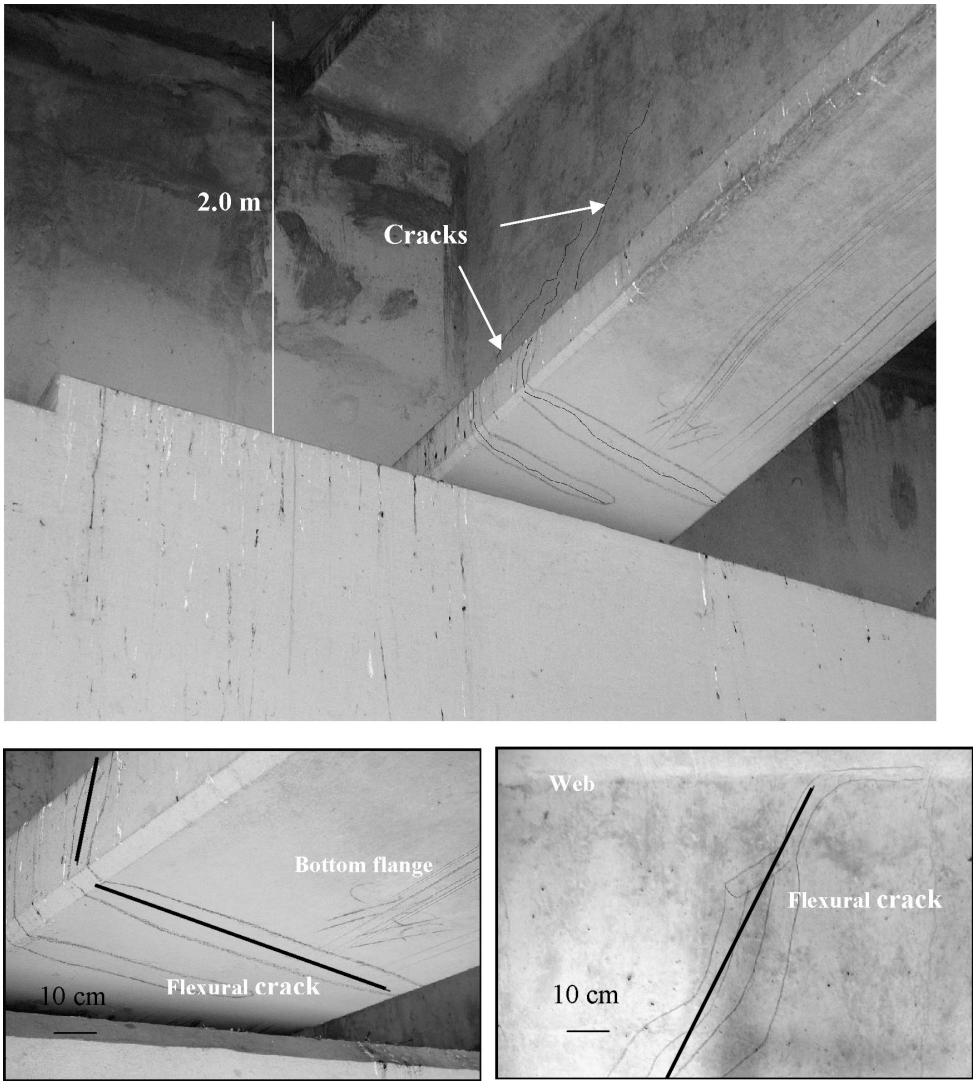


**Figure 4.** Initial cracks in analyzed girder, flexural cracks in flange and shear crack in the web (black lines illustrate crack direction).

### *3.2. Preliminary repair*

As shown in Fig. 5, some preliminary repair implemented by injecting polyurethane foam in the cracks is seen to be ineffective in containing the growth of stress- and environment-induced cracks. This technology only seals the crack. By sealing the cracks no infusion of resin can take place inside the cracks. No actual improvement is achieved in the structural integrity to carry the imposed load coming from the deck. Crack propagation is still in the micro phase. In order to improve this situation one must not only seal the cracks but also stop the crack propagation.

**Table 1.**
Average seasonal temperature in Huntsville, Alabama, USA*

| | Huntsville | |
|---|---|---|
| | High | Low |
| Spring | 74/23 | 50/10 |
| Summer | 92/33 | 69/20 |
| Fall | 75/24 | 50/10 |
| Winter | 53/12 | 34/01 |
| Mean Annual | 73/23 | 50/10 |

All temperatures given in Fahrenheit/Celsius.

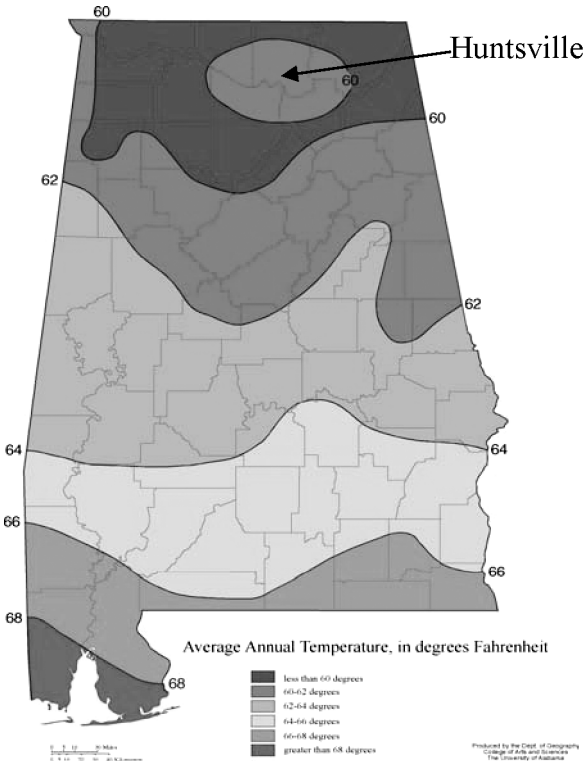


* Source: http://www.netstate.com/states/geography/al_geography.htm

### *3.3. Experimental program*

A characterization study was undertaken first at the University of Alabama at Birmingham laboratory to investigate strength of existing girders in comparison to the VARTM repaired/strengthened samples. For screening and identification of potential solution, two types of concrete specimens were fabricated. One was a small prism 101.6 mm × 76.2 mm × 406.4 mm (4″ × 3″ × 16″) and the other was a 152.4 mm × 304.8 mm × 1828.8 mm (6″ × 12″ × 72″) reinforced concrete beam. Small prisms were used to investigate the bond strength and interface properties between the concrete and CFRP. The large specimens were used to investigate the load carrying capacity while reinforced with the same CFRP and epoxy resin system. The work was done according to the test matrix given in Table 2 and Table 3. Detailed results are presented in Uddin *et al*. [7].

**Figure 5.** Some preliminary repair implemented by injecting polyurethane foam in the cracks is seen to be ineffective at I-565 highway bridge girder in Huntsville.

**Table 2.**
Test matrix small beam (1st phase)

| Treatment | No. of prisms in tilt/out of plane de-bonding | No. of prisms in in-plane | No. of prisms in pull-off test | Prism size, mm (inch) |
|---|---|---|---|---|
| Smooth as it is | 3 | 3 | 3 | 101.6 × 76.2 × 406.4 (4 × 3 × 16) |
| Smooth/Micro balloon synthetic | 3 | 3 | 3 | 101.6 × 76.2 × 406.4 (4 × 3 × 16) |
| Smooth/Primer/ Functional group | 3 | 3 | 3 | 101.6 × 76.2 × 406.4 (4 × 3 × 16) |
| Sand blasting/ Wire blasting | 3 | 3 | 3 | 101.6 × 76.2 × 406.4 (4 × 3 × 16) |
| Surface washing | 3 | 3 | 3 | 101.6 × 76.2 × 406.4 (4 × 3 × 16) |

### *3.4. Pull-off test*

The surface strength of the concrete was studied by pull-off tests [7]. From Table 2, it was seen that sandblasting treatment was effective in transferring higher loads through the bond. Figure 6 shows a summary of the pull-off test results. So it was decided that the second phase of the test would only be conducted with the sand blasting surface treatment.

**Table 3.**
Large beam specimens (2nd phase)

| Beam No. | Beam description | Test procedure (four-point bending) and failure mode | Beam dimensions, mm (inch) |
|---|---|---|---|
| 1 | Virgin (FV-Control) | Full or partial failure in flexure | $152.4 \times 304.8 \times 1828.8$ $(6 \times 12 \times 72)$ |
| 2 | Virgin + Tensile face reinforced (FVVTM) | Full failure in flexure | $152.4 \times 304.8 \times 1828.8$ $(6 \times 12 \times 72)$ |
| 3 | Partial failure repair with CFRP (FPVTM) | Full failure in flexure | $152.4 \times 304.8 \times 1828.8$ $(6 \times 12 \times 72)$ |

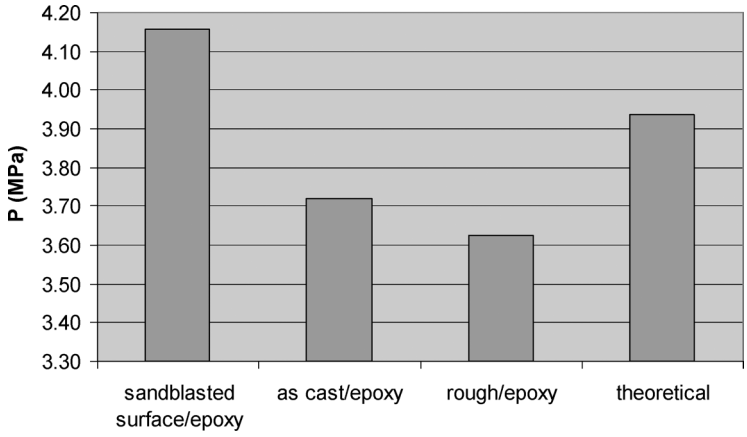


**Figure 6.** Results from pull-off test.

### *3.5. In-plane shear test*

The interface developed using VARTM between concrete substrate and the carbon fabric was studied based on the model of similar to the test apparatus of in-plane shear used by Bizindavyi and Neale [8]. The schematic of this model has been shown in Fig. 7. The assembly is supported in such a way that there is direct shear at the composite-to-concrete interface. This test set-up is an adequate way of determining the bond length as well as the general properties and behavior of the formed interface under the chosen conditions of surface preparation and processing. The analytical models developed by Hiroyuki and Wu [9], Neuerbauer and Rostasy [10], Tanaka [11], Volnyy and Pantelides [12] confirm this experimental in-plane shear test.

In this test a uni-axial tension is applied on the fabric bonded to the concrete, so that the interface is subjected to pure shear. It is known that the application of a laminate to a concrete beam introduces shear transfer to the concrete/epoxy interface. Figure 8 compares experimental VARTM results with the analytical model [7].

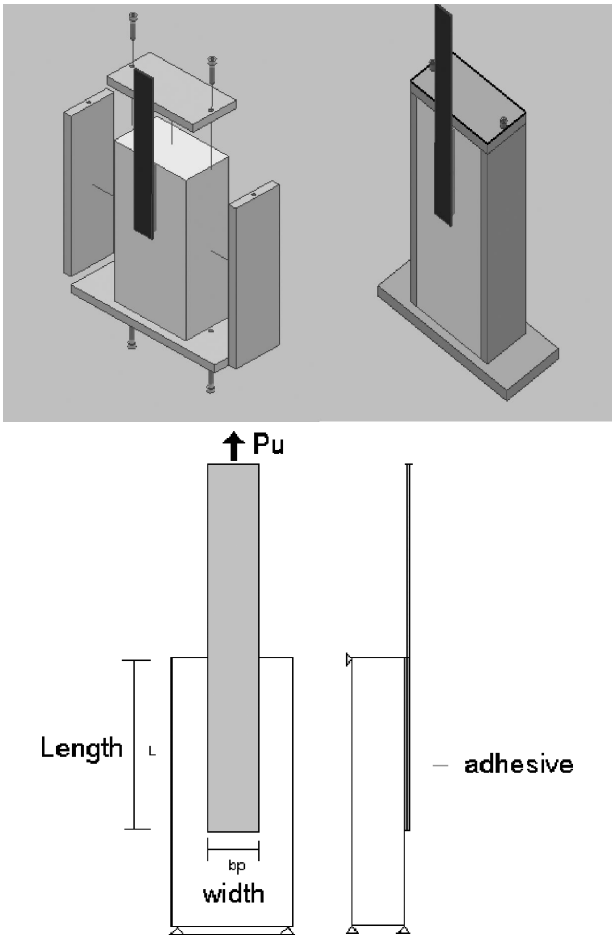


**Figure 7.** In-plane shear test schematic.

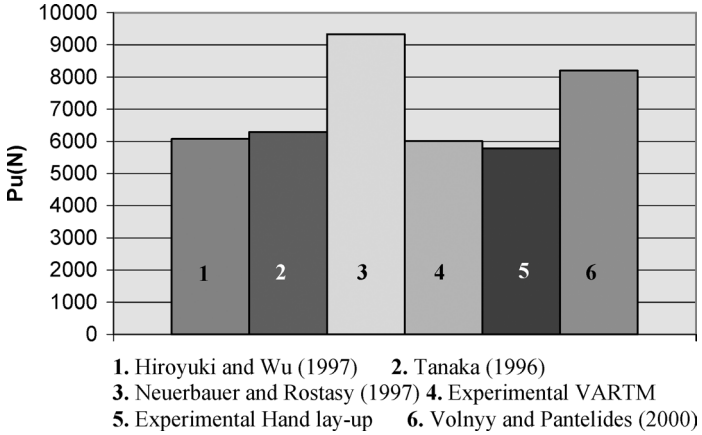


**Figure 8.** Experimental and theoretical results of in-plane shear test.

**Table 4.**
FRP reinforcement characteristics and surface preparation

| Beam code/Beam No. | Surface preparation | Beam condition | CFRP strengthening |
|---|---|---|---|
| FV-Control (1) | None | Virgin | None |
| FVVTM (2) | Sand blasting | Virgin | One ply |
| FPVTM (3) | None | Pre-cracked | One ply |

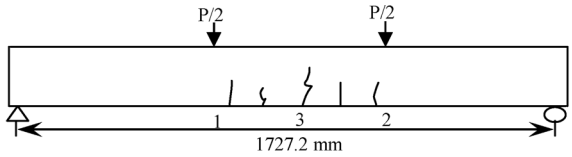


Fig (8-a): FV -Control Beam

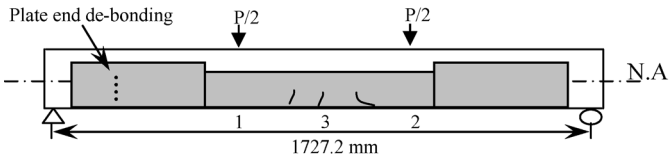


Fig (8-b): FVVTM Beam

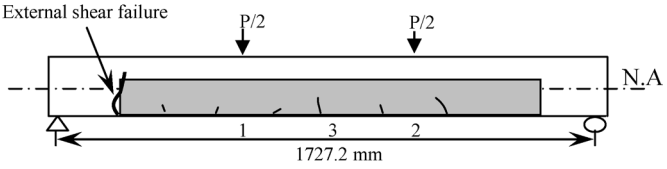


Fig (8-c): FPVTM Beam

1, 2, and 3 are strain gauge locations

**Figure 9.** Strengthening scheme and failure modes.

### *3.6. Beam test and instrumentation*

In the second phase of the experiment, the beams numbered 1, 2 and 3 are called Control, FVVTM and FPVTM beams, respectively. The first letter (F) indicates the way of testing the beam to be failed, here flexure, the second letter (V or P) indicates the beam condition, virgin or pre-cracked, and the third one (VTM) indicates the VARTM strengthening technique. In Table 4, reinforcement characteristics and surface preparation of the three beams are shown.

Schematics of failure mode and FRP strengthening scheme for all three beams are shown in Fig. 9. A Linear Variable Displacement Transducer (LVDT) was placed under the mid span of the beam to measure the deflection, two strain gauges were

attached beneath the point load location and one was attached at the mid span of the beam, as shown in Fig. 9 (1, 2, and 3 are strain gage locations). All three strain gages were attached at the tension face of the beam. The strain gauges and the LVDT were connected to a data acquisition system (MEGADAC) which records data every one second. The load was applied through a load cell which was placed on the top of the set-up.

### *3.7. Experimental results and analysis*

These tests were done to study the behavior of VARTM strengthening RC beam under flexural condition. Typical load *versus* deflection curves for three types of beam are shown in Figs 10 and 11. Table 5 shows the load, deflection and failure mode of the three tested beams. Figure 10 shows the load–deflection curve of FV-control and FVVTM beams. The FVVTM beam shows higher ultimate load before failure, compare to the unstrengthened beam (Fig. 10). Figure 11 shows the load–deflection curve of a pre-cracked beam. From the figure it is seen that the ultimate load was increased significantly after the VARTM strengthening. The tested RC beams were designed to balance failure so cracks at the bottom face and crushing in compression side in FV-Control beams confirms this. For the FVVTM beam, as both flexure and shear reinforcement were used, debonding occurred at the flexural CFRP plate cut-off point. For the FPVTM beam, no external reinforcement for shear had been done, so external shear failure was observed along with concrete crushing for this case.

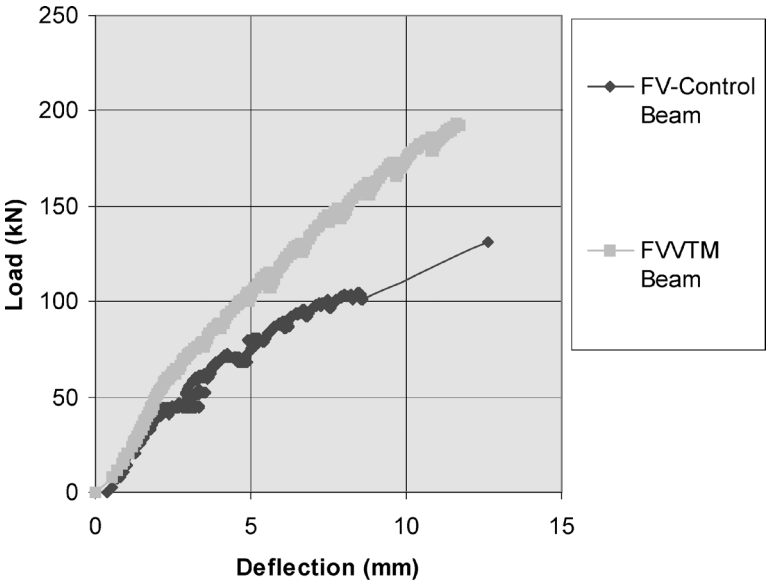


**Figure 10.** Load *vs* mid-deflection curve of FVVTM and FV-control beam.

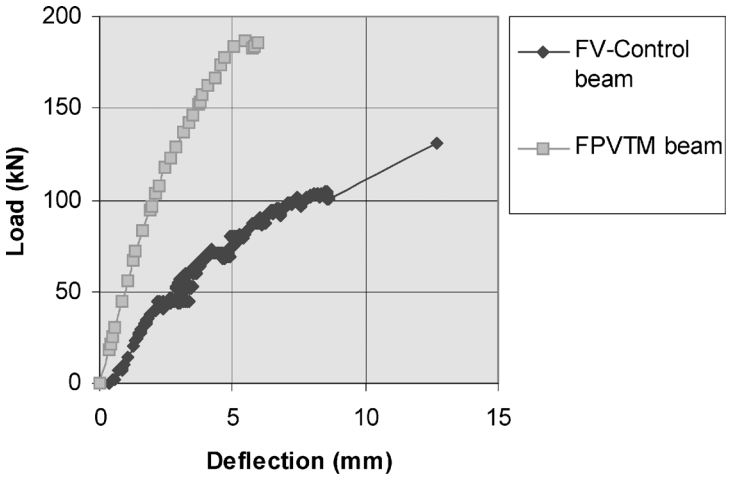


**Figure 11.** Load *vs* mid-deflection curve of FPVTM beam before and after VARTM strengthening.

**Table 5.**
Load, deflection and failure mode of tested beam

| Beam | Failure load, kN (kip) | Deflection, mm (inch) | Failure mode |
|---|---|---|---|
| FV-control | 129.4 (29.4) | 12.45 (0.49) | Flexure failure |
| FVVTM | 187.54 (43.32) | 11.71 (0.46) | Out of plane debonding |
| FPVTM | 185.54 (43.35) | 6.15 (0.24) | Shear |

## 4. CFRP DESIGN CALCULATION

The cross-section of the 1600.2 mm (63″) bulb-tee girder is shown in Fig. 12. Table 6 shows the sectional properties of the 1600.2 mm (63″) bulb-tee girder. Table 7 shows the sectional properties of 1600.2 mm (63″) bulb-tee girder and 203.2 mm (8″) cast-*in-situ* slab. Here it was assumed that after developing flexural cracks, the concrete section is fully cracked and the concrete is no longer able to carry any tensile force. To retrofit such a section, it was assumed that the external reinforcement carries all of the nominal capacity of the section. The first critical section was calculated as $h_c$, centroid of the pre-stressing + 254 mm (10″), i.e. $h_c$ + 254 mm ($h_c$ + 10″) from the support. At this critical section both the pre-stressing force and temperature variation were considered in calculating the required number of CFRP layers. All the calculations for the required CFRP have been shown in Table 8 to Table 11. From Table 11, two layers of CFRP were required for flexural reinforcement. In order to avoid shear failure, shear reinforcement was calculated based on 292.6 kN (65.7 kips) shear force developed at the critical section from the load of an HS 20 truck. Based on the design guidelines ACI 440 [13], this gave two layers of CFRP for shear strengthening of that section. These shear

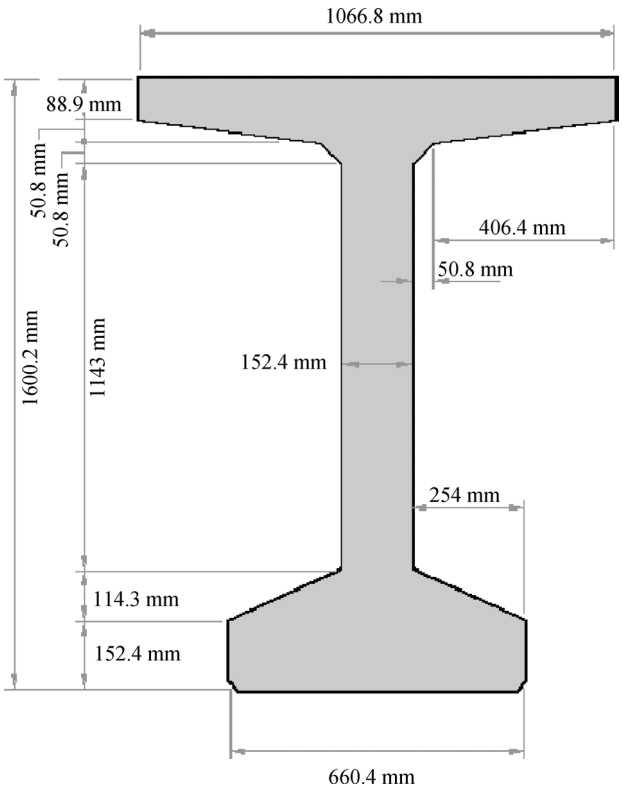


**Figure 12.** The cross-section of bulb T-girder.

**Table 6.**
Bulb T-girder sectional properties

| Girder type | Beam height mm (in) | Web height mm (in) | Section area $mm^2$ ($in^2$) | Center of gravity mm (in) | Moment of inertia $mm^4$ ($in^4$) | Weight N/mm (lb/ft) | Max. span* mm (ft) |
|---|---|---|---|---|---|---|---|
| BT-63 | 1600.2 (63) | 1143 (45) | 459999.08 (713) | 815.848 (32.12) | $1.6343 \times 10^{11}$ (392,638) | 10.85 (743) | 3302 (130) |

* Based on simple span, HS-25 loading and $f_c' = 48.3$ MPa (7000 psi).

reinforcements were placed along with the flexural reinforcement as a 0/90/0/90 sequence.

### *4.1. VARTM in I-565 highway bridge girder: Processing detail*

After performing strengthening calculations, two flexure layers and two shear layers of unidirectional carbon fiber, and epoxy resin were selected for retrofitting the T-bulb girder. Retrofitting strategy and schematic of process detail is shown in Figs 13, 14 and 15. A crew of four students carried out processing on site for a period of

**Table 7.**
Sectional properties of 63″ bulb T-girder and 8″ cast *in situ* slab

| Element | A<br>$mm^2$<br>($in^2$) | Y<br>mm<br>(in) | AY<br>$mm^3$<br>($in^3$) | $AY^2$<br>$mm^4$<br>($in^4$) | $I_0$<br>$mm^4$<br>($in^4$) | $I_{gc}$<br>$mm^4$<br>($in^4$) |
|---|---|---|---|---|---|---|
| Slab | 348644.4<br>(540.4) | 1682.75<br>(66.25) | 586681311.1<br>(35801.49) | $9.87238 \times 10^{11}$<br>(2371848.72) | 791945973.6<br>(1902.66) | $9.88 \times 10^{11}$<br>(205601.04) |
| Girder | 459999.1<br>(713) | 815.848<br>(32.12) | 375289329.4<br>(22901.56) | $3.06179 \times 10^{11}$<br>(735598.11) | $1.63428 \times 10^{11}$<br>(392638) | $1.63 \times 10^{11}$<br>(547025.9) |
| Total | 808643.4<br>(1253.4) | | 961970640.5<br>(58703.05) | $1.29342 \times 10^{11}$<br>(3107446.83) | $1.6422 \times 10^{11}$<br>(394540.7) | $1.15 \times 10^{11}$<br>(752626.94) |

**Table 8.**
Pre-cast AASHTO 1600.2 mm (63″) bulb T-girder properties

| Pre-cast beam | Composite beam<br>(with transformed slab) |
|---|---|
| $A_c = 459999.08$ $mm^2$ (713 $in^2$) | $A_{cc} = 808643.4485$ $mm^2$ (1253.4 $in^2$) |
| $y_t = 784.352$ mm (30.88 in) | $y_{tc} = 14622.51633$ mm (22.67 in) |
| $y_b = 815.848$ mm (32.12 in) | $y_{bc} = 1189.610381$ mm (46.84 in) |
| $h = 1600.2$ mm (63 in) | $h_c = 1765.3$ mm (69.5 in) |
| $I_g = 1.63428 \times 10^{11}$ $mm^4$ (392638 $in^4$) | $I_{gc} = 3.13267 \times 10^{11}$ $mm^4$ (752626.9 $in^4$) |
| $Z_t = 208360882$ $mm^3$ (12714.96 $in^3$) | $Z_{tc} = 544159517.9$ $mm^3$ (33206.65 $in^3$) |
| $Z_b = 200317062.1$ $mm^3$ (12224.1 $in^3$) | $Z_{bc} = 263335787$ $mm^3$ (16069.74 $in^3$) |
| $k_t = -435.4727451$ mm (−17.14 in) | $k_{tc} = -325.651296$ mm (−12.82 in) |
| $k_b = 452.959345$ mm (17.83 in) | $k_{bc} = 672.9288649$ mm (26.49 in) |
| $b_v = 1066.8$ mm (42 in) | $h_f = 165.1$ mm (6.5 in) |
| $b_w = 152.4$ mm (6 in) | $b_e = 2438.4$ mm (96 in) |
| | $b = b_{tr} = 2111.716345$ mm (83.14 in) |

two days on a 1.52 m × 4 m area. The first step in the processing was the surface preparation of the girder using a sandblaster and compressed air; after the surface cleaning, a coat of resin was applied in the border of the part to ensure an adequate seal between the concrete and the vacuum sealant tape as shown in Fig. 16.

After the layer of primer was cured, the vacuum sealant tape was placed onto the surface of the concrete following the pattern of the part to be bagged. The lay-up sequence of [0/90/0/90] was adopted and the flexure plies were laid first in order to have the shear plies (laid up to 0.2 m above the neutral axis to ensure anchoring effects) helping in containing the edge peel stresses that usually initiate debonding of the flexure plies. All plies were held in place against the concrete surface with the aid of 3M-spray adhesive as shown in Fig. 17. Once all the plies were in place, a porous bleeder release film made of tightly woven silicone coated polyester was placed on top of the lay up so that the distribution mesh would not bond to the fabric (Fig. 18).

**Table 9.**
Bending moments and shear forces for a typical beam

| Element | Magnitude | Unit | Location |
|---|---|---|---|
| Weight of pre-cast beam | 10.8<br>(0.74) | N/mm (klf) | |
| Weight of the slab | 9.5<br>(0.65) | N/mm (klf) | |
| Super imposed dead load | 3.5<br>(0.25) | N/mm (klf) | |
| HS20 truck P | 71200<br>(16) | N<br>(kip) | |
| Moment due to single loading lane | 1808869<br>(1330.1) | N m<br>(kips-ft) | |
| $M_{\text{lane}}$ | 1808869<br>(1330.1) | N m<br>(kips-ft) | at mid span |
| D.F | 1.45 | | |
| I | 0.23 | | |
| $M_{\text{L+I}}$ | 1622619.0<br>(1193.1) | N m<br>(kips-ft) | |
| First critical section | 1009.65<br>(3.313) | Mm<br>(ft) | from support |
| $V_{\text{lane}}$ | 274978.7<br>(61.8) | N<br>(kips) | |
| $V_{\text{L+I}}$ | 246665.5<br>(55.4) | N<br>(kips) | |

**Table 10.**
Moment and shear force

| Loading | Moment at midspan N m (kips-ft) | Shear forces at first critical section N (kips) | Moment at first critical shear section N m (kips-ft) | Resisting section |
|---|---|---|---|---|
| Precast beam | 1004679.1<br>(738.7) | 136462.5<br>(30.7) | 143690.8<br>(105.7) | Precast |
| Cast on place slab | 879270.3<br>(646.5) | 119428.6<br>(26.8) | 125062.9<br>(92) | |
| $M_{\text{p}}$ | 1883949.4<br>(1385.25) | 255891.1<br>(57.5) | 268753.6<br>(197.6) | |
| Asphalt | 338180.9<br>(248.7) | 45934.1<br>(10.32) | 48367.2<br>(35.6) | Composite |
| Live load + impact | 1622619.0<br>(1193.1) | 246665.5<br>(55.4) | 278377.3<br>(204.9) | |
| $M_{\text{c}}$ | 1960799.9<br>(1441.8) | 292599.6<br>(65.7) | 326744.4<br>(240.3) | |

**Table 11.**
Number of CFRP layers calculation

| Area/No. of CFRP layer | Nominal moment capacity | For temperature | At critical section | |
|---|---|---|---|---|
| | | | Temperature and pre-stressing effect | Shear force for HS 20 truck |
| Required area of CFRP $A_f$ mm$^2$ (in$^2$) | 11548.4 (17.9) | 1871 (2.9) | 4839 (7.5) | 890.3 (1.38) |
| No. of layers of CFRP | 3.4 | 0.47 | 1.42 | 1.72 |
| Remarks (CFRP need) | 4 | 1 | 2 | 2 |



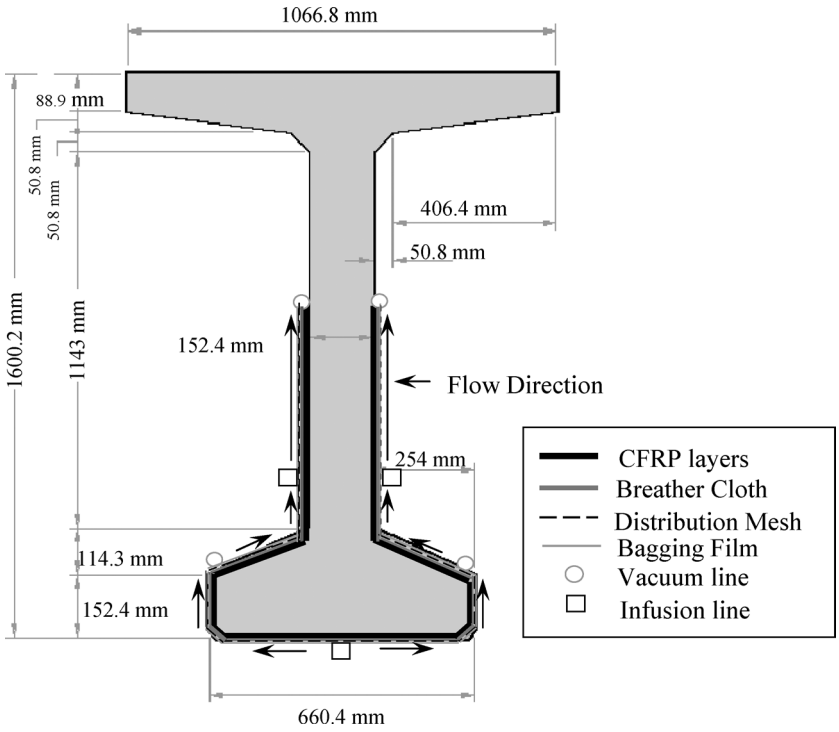


**Figure 13.** Schematic of bulb T-section with retrofitting strategy.

Then the distribution mesh, made from polyethylene terephthalate (PET) was placed with the infusion and vacuum lines on the top of the plies and on the upper part of the bottom flange. Following the placement of the distribution mesh and the inlet and outlet channels, the bag was put in place on top of the whole arrangement

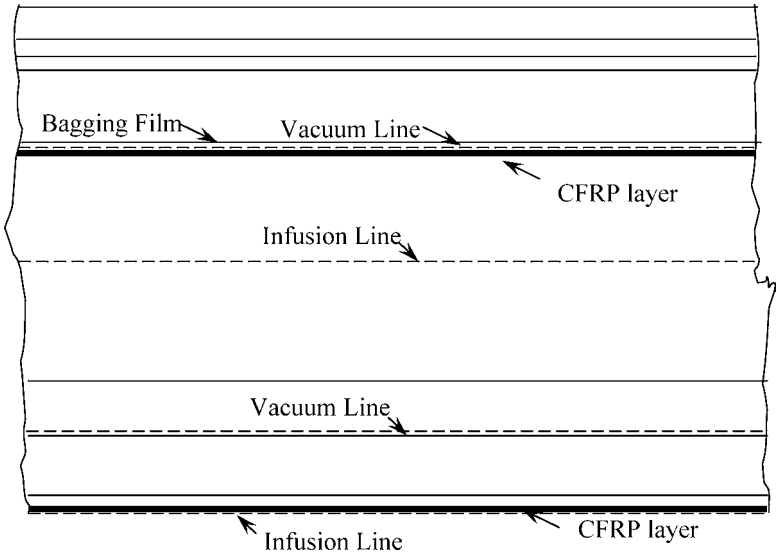


**Figure 14.** Longitudinal view of the 1600.2 mm (63″) bulb T-girder (not in scale).

as illustrated in Fig. 19. Debulking took place for 20 min under vacuum, and the bag was straightened and checked for leaks.

The infusion strategy proposed was placing an infusion channel at the middle of the bottom flange, two infusion/vacuum channels at the web and bottom flange and two final vacuum channels at the top of the part in the web as seen in Fig. 13. Finally, infusion was performed and monitored for 90 min; the flow front was very homogeneous and symmetrical to each side of the girder showing a linear pattern. The part was kept under vacuum for the following 12 h to ensure proper curing under 635 mmHg vacuum pressure (Fig. 20). The on-site filling time for the girder was approximately 60 min. After debagging, the part had conformed readily to the shape of the girder; details of the web and beam appearance at debagging are presented in Fig. 21. A coat of latex based paint was applied on the surface of the finished part to act as a seal against any environmental attack such as moisture, dust or particles (Fig. 22) and a final overall view is shown in Fig. 23.

## 5. COST EVALUATION FOR FIELD IMPLEMENATION OF VARTM

A generalized analysis of the main factors influencing the economics of the process was performed by Juan [14] and the total price for the initial stage of the project was estimated using three different processing techniques: VARTM, hand lay-up and steel plate bonding. The total initial cost for the project for repair of 6.4 $m^2$ (Table 12 and Fig. 24) was found to be lower for the case of steel plate bonding. However, maintenance costs and durability of the bonded steel plates in terms of corrosion and bond line degradation increase the overall cost of using steel. Another

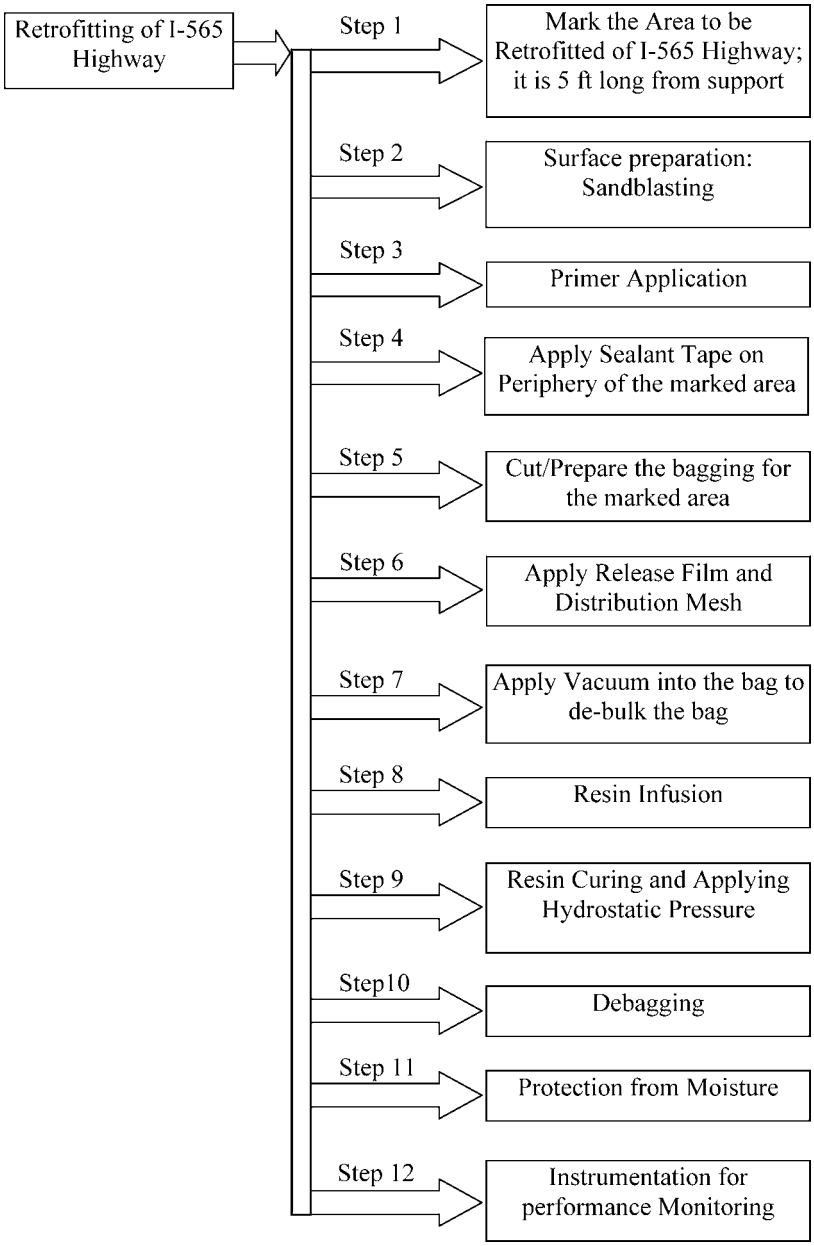


**Figure 15.** Schematic of retrofitting scheme of I-565 Highway bridge at a glance.

important issue to take into consideration is that, when a long span is going to be repaired, steel plates need to be welded in place and thereby welding labor, machinery and consumables increase cost. These combined facts make the use of composite materials more attractive, competitive and permanent. Hand lay-up and VARTM are very similar in terms of costing, since the relatively higher tooling cost

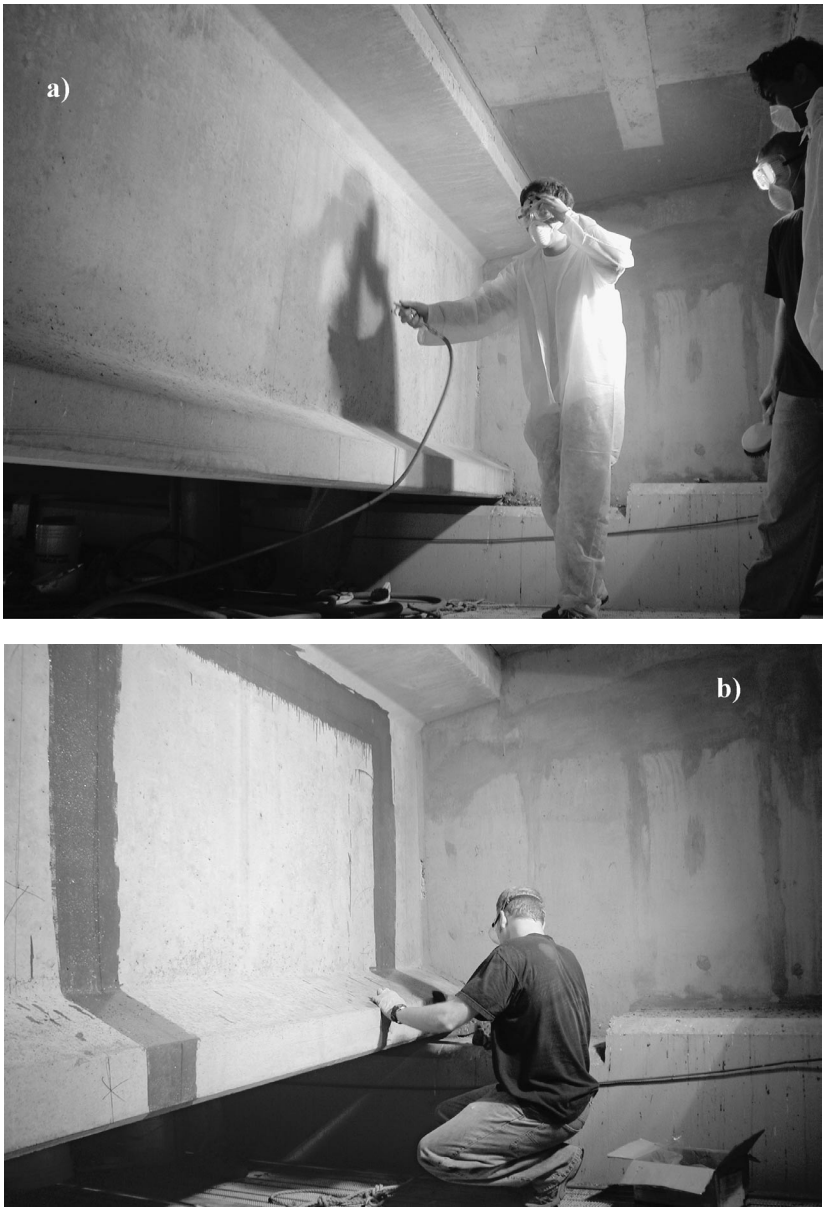


**Figure 16.** (a) Surface preparation and (b) pre-priming of vacuum bag sealant tape zone.

in VARTM is equivalent in the hand lay-up process by the increased labor rates and longer processing times. The advantages of the final VARTM product over hand lay-up (e.g. higher quality product, which might help reduce the number of layer needed and improved bond and durability [14]) make it an attractive, cost effective processing route for the repair of large reinforced concrete structures.

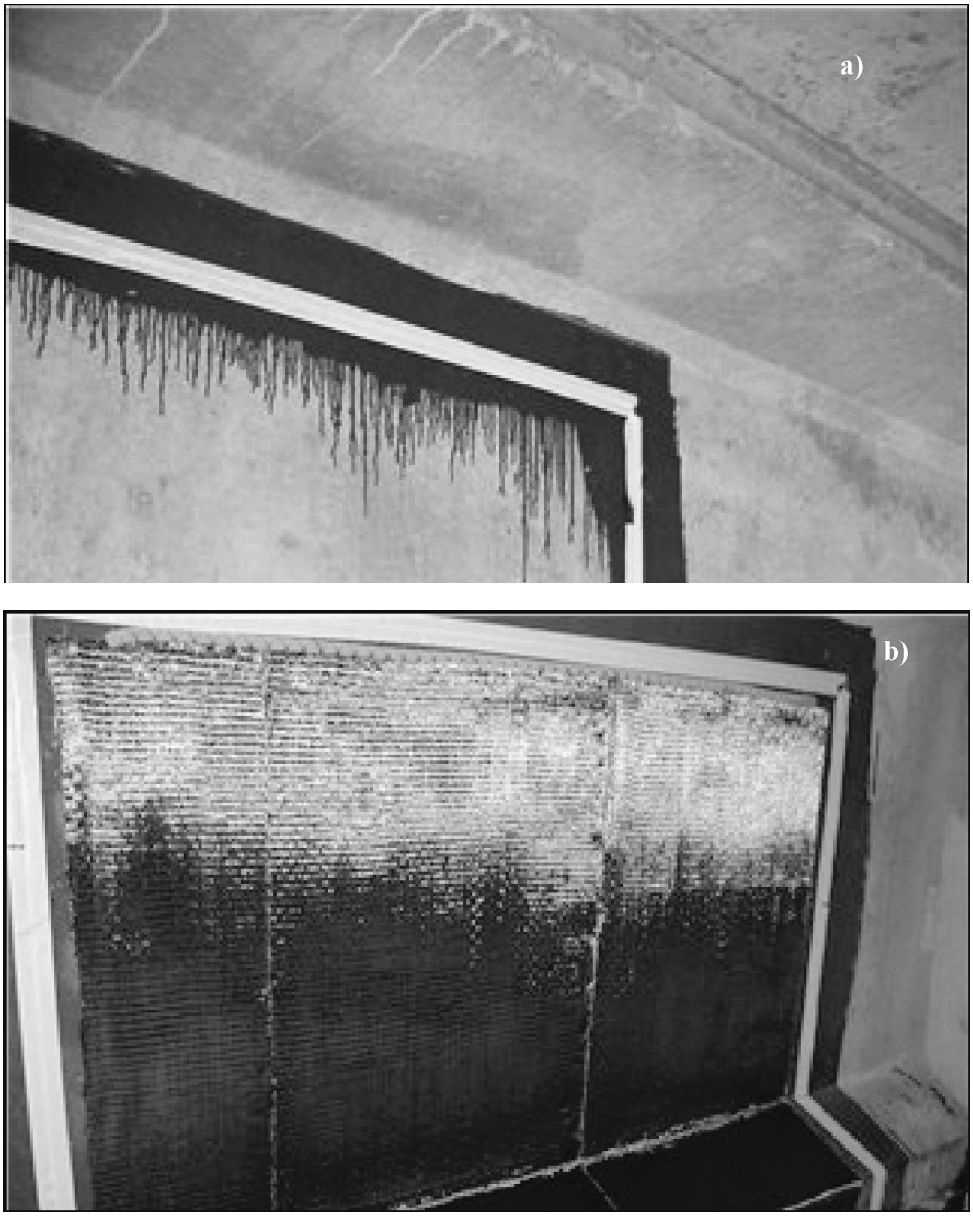


**Figure 17.** (a) Sealant tape lay out and (b) fabric placement with 3M spray adhesive.

## 6. CONCLUSION

Cost effective methods with potential for field implementation are necessary to address the issue of repair and vulnerability of bridge structures. Most infrastructure related applications of fiber-reinforced plastics (FRPs) use traditional hand lay-up technology. The hand lay-up is tedious, expensive, labor-intensive and prone to


**Figure 18.** (a) Release film and (b) distribution mesh placement over placed fabric.

personnel skill level. A major disadvantage of the wet lay-up technique, even when combined with vacuum bagging, is that proper compaction of the fabric is not achieved. Moreover, for rehabilitation of large-civil structures, affordability and practicality are of prime concern.

In the work presented here, the investigation addresses a newly emerging liquid molding technique referred to as vacuum assisted resin transfer molding (VARTM).

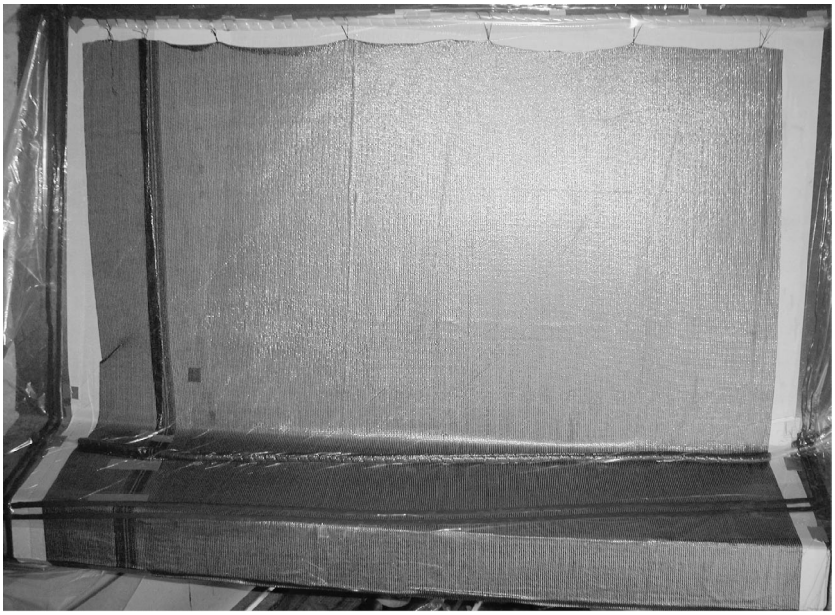

**Figure 19.** Bagging and debulking of lay-up.

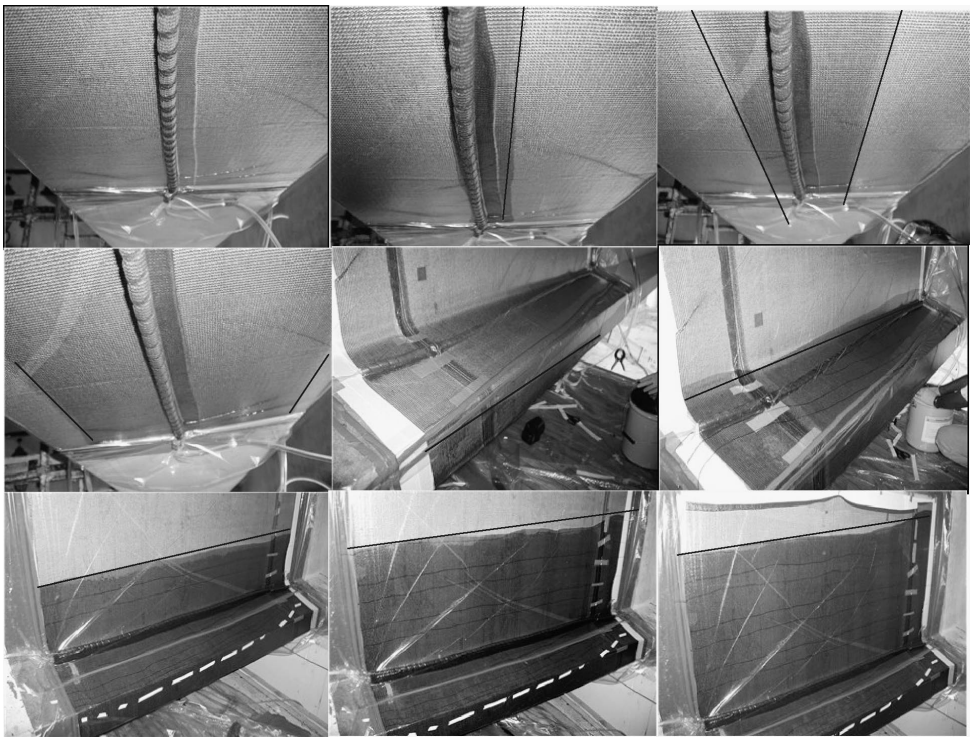

**Figure 20.** Infusion progression and flow front throughout flange and web. Straight line indicates flow front. Dark areas indicate wet area, light grey represents dry areas.

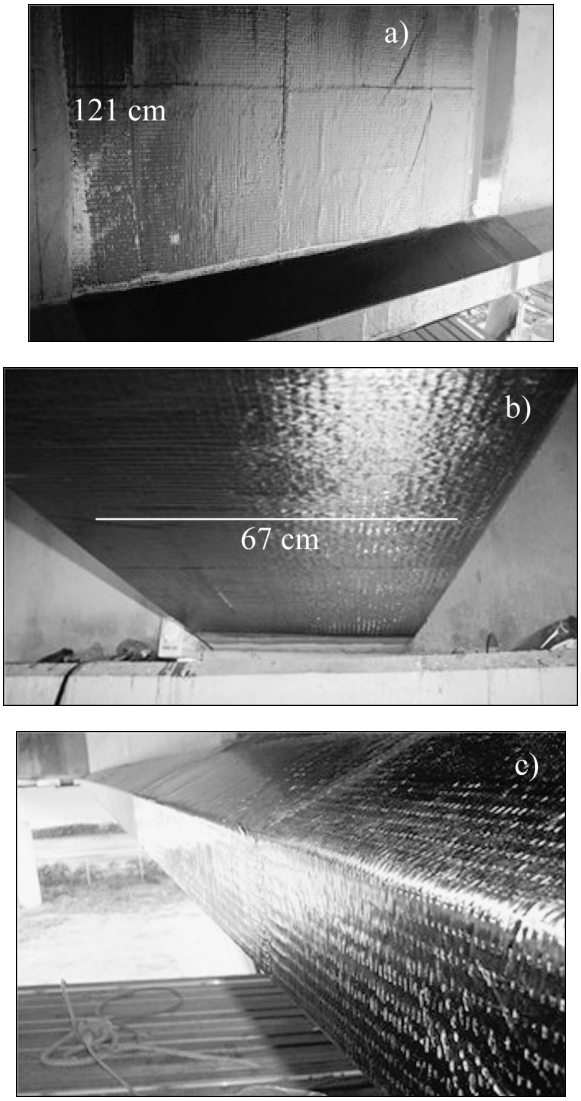


**Figure 21.** (a) Part after debagging; (b) bottom flange detail and (c) bottom flange side detail.

**Table 12.**
Initial project cost for repair of 6.4 $m^2$ of concrete girder using three different processing approaches

| | VARTM | Hand lay-up | Steel plate bonding |
|---|---|---|---|
| Variable cost | 1260 | 1110 | 1750 |
| Direct labour | 3648 | 4320 | 1860 |
| Material | 4620 | 4620 | 884 |
| Tooling | 269.8 | 80 | Not applicable |
| Total cost | 9797.8 | 10130 | 4494 |

**Figure 22.** Latex based coating application.

**Figure 23.** Final overall view of reinforced section.


**Figure 24.** Initial project cost for repair of 6.4 $m^2$ of concrete girder using three different approaches.



It is a promising low-cost innovation to traditional composite manufacturing methods. It uses single-sided tooling (translating to significant savings in tooling costs) and vacuum-bag technology. Laboratory experiments were performed first to optimize the processing parameters, and material types (fabric and resin) to be adopted in retrofitting existing structures. In-plane shear bonding test showed that VARTM can generate a strong interface between composite laminate and the conditioned surface of the concrete indicating the feasibility of VARTM for bonding composite laminate to concrete surfaces. VARTM was then implemented in a laboratory scale for the repair and upgrade of reinforced concrete rectangular beams, showing a considerable increase in capacity as compared to the unreinforced section and a over wider variety of failure mechanisms. Finally, this newly introduced technique was successfully implemented in the field for the repair of pre-cracked reinforced concrete T-bulb I-565 highway bridge girder in Huntsville, Alabama within two days without any traffic interruption.

This process has very attractive cost-advantages in comparison to spray-up or hand lay-up impregnation methods, and it is far less expensive than conventional repairing methods. An economical analysis showed that VARTM is a competitive route for reinforcing large structures; the overall cost for the project was estimated and compared with traditional methods. Initial project costs were very similar when compared to the use of hand lay-up techniques and about three times more expensive than the use of conventional steel plate bonding. However, life cycle expectancy and maintenance costs were not taken into account and can ultimately give competitive advantage to VARTM over steel plate bonding and hand lay-up.

*Acknowledgements*

The authors gratefully acknowledge funding and support provided by Alabama Department of Transportation (ALDOT) research project 930-549, under guidance of Bridge Engineers Mr. Fred Conway and George Connor, and Robert King of Federal Highway Administration (FHWA).

## REFERENCES


1. R. Mayo, A. Nanni, W. Gold and M. Baker, Strengthening of bridge G270 with externally bonded carbon fiber reinforced polymer reinforcement, SP-188, in: *American Concrete Institute Proceedings of the Forth International Symposium on FRP for Concrete Structures (FRPRCS4),* Baltimore MD, USA, pp. 429–440 (1999).
2. D. Kachlekev and M. Laylor, *FRP Composite for Strengthening Bridges in Oregon*. Oregon Department of Transportation (2000).
3. M. B. Shahrooz and S. Boy, *Retrofitting of Existing Reinforced Concrete Bridges with Fiber Reinforced Polymer Composites*. Ohio Department of Transportation and the U.S. Department transportation, Federal Highway Administration, Report No. UC-CII 01/01 (2001).
4. W. D. Brouwer, E. C. F. C. Van Herpet and M. Labordus, Vacuum injection moulding for large structural applications, *Composites Part A: Appl. Sci. Manufacturing* **34**, 551–558 (2003).
5. N. L. Han, S. S. Suh, J. M. Yang and H. T. Hahn, Resin film infusion of stitched stiffened composite panels, *Composites. Part A: Appl. Sci. Manufacturing* **34**, 227–236 (2003).
6. N. Uddin, U. K. Vaidya, M. Shohel and J. C. Serrano-Perez, *ALDOT Research Project # 930-549*. Alabama Department of Transportation (2003).
7. N. Uddin, U. K. Vaidya, M. Shohel and J. C. Serrano-Perez, In-plane debond response of vacuum assisted resin transfer molded carbon fiber sheets on concrete substrates, *Cement Concrete Composites* (submitted).
8. L. Bizindavyi and K. W. Neale, Transfer length and bond strengths for composites bonded to concrete, *J. Compos. Construction ASCE* **3** (4), 153–160 (1999).
9. Y. Hiroyuki and Z. Wu, Analysis of debonding fracture properties of CFS strengthened member subject to tension. in: *Non-metallic (FRP) Reinforcement for Structures, Proc. 3rd Intern. Symp.*, Sapporo, Japan, pp. 287–294 (1997).
10. U. Neuerbauer and F. S. Rostasy, Design aspects of concrete structure strengthened with externally bonded CFRP plates, in: *Proc. 7th Intern. Conf. on Structural Faults and Repairs*, M. C. Forde (Ed.), pp. 109–118 (1997).
11. T. Tanaka, Shear resisting mechanism of reinforced concrete beams with CFS as shear reinforcement, Graduation Thesis, Hokkaido University, Japan (1996).
12. V. A. Volnyy and C. P. Pantelides, Bond length of CFRP composites attached to precast concrete walls, *J. Compos. Construction* **3** (4), 168–176 (1999).
13. American Concrete Institute, *Guide for the Design and Construction of Externally Bonded FRP System for Strengthening Concrete Structures*. ACI committee 440 (2000).
14. J. C. Serrano-Perez, Implementation of vacuum assisted resin transfer molding in the repair of reinforced concrete structures, Masters of Science Thesis, University of Alabama at Birmingham, USA (2003).